We are IntechOpen, the world's leading publisher of Open Access books
Built by scientists, for scientists

4,800
Open access books available

122,000
International authors and editors

135M
Downloads

Our authors are among the

154
Countries delivered to

TOP 1%
most cited scientists

12.2%
Contributors from top 500 universities

CLARIVATE ANALYTICS
BOOK CITATION INDEX
INDEXED

WEB OF SCIENCE™

Selection of our books indexed in the Book Citation Index in Web of Science™ Core Collection (BKCI)

Interested in publishing with us?
Contact book.department@intechopen.com

Numbers displayed above are based on latest data collected.
For more information visit www.intechopen.com

Chapter 8

Milliwatt-Level Electromagnetic Induction-Type MEMS Air Turbine Generator

Minami Kaneko, Ken Saito and Fumio Uchikoba

Additional information is available at the end of the chapter

http://dx.doi.org/10.5772/intechopen.74830

Abstract

In this chapter, an electromagnetic induction-type MEMS air turbine generator that combined with the MEMS technology and the multilayer ceramic technology is proposed. Three types of MEMS air turbine generators that included the different bearing systems, shape of the rotor and shape of the magnetic circuits are discussed to achieve the high output power. In the MEMS air turbine, the purpose is to achieve high-speed rotational motion. As a result of the comparison between the different structures, a rim-type rotor and a miniature ball bearing system showed the high rotational speed than a flat-type rotor and a fluid dynamic bearing system. The maximum rotational speed of the fabricated air turbine was 290,135 rpm. Moreover, it is important to introduce the magnetic flux to the magnetic circuit. By the multilayer ceramic technology, the three-dimensional coil in miniature monolithic structure was fabricated. The magnetic core that was designed to introduce the magnetic flux showed the low magnetic flux loss. The fabricated MEMS air turbine and the multilayer ceramic magnetic circuit were combined, and the miniature electromagnetic induction-type generator was achieved. The output power was 2.41 mVA, when the load resistance and the output voltage were 8 Ω and 139 mV, respectively.

Keywords: electromagnetic induction type, multilayer ceramic technology, air turbine generator, ferrite, milliwatt level

1. Introduction

Micro elector mechanical systems (MEMS) are used for various fields. The most conventional field is a miniature electronics field as sensors. These are made from single-crystal silicon. Characteristics of the MEMS are a fine pattern, a high accuracy, and a high-aspect

IntechOpen

© 2018 The Author(s). Licensee IntechOpen. This chapter is distributed under the terms of the Creative Commons Attribution License (http://creativecommons.org/licenses/by/3.0), which permits unrestricted use, distribution, and reproduction in any medium, provided the original work is properly cited. CC BY

ratio. MEMS process is based on the integrated circuit (IC) production process, and it can form a fine pitch pattern on a planer silicon structure. Moreover, the high accuracy and the high aspect ratio pattern are realized by a Bosch process [1]. By this process, it is possible to form miniature mechanical parts and fabricate an acceleration sensor, a gyroscope sensor, and so on. The miniature sensors progress a miniaturization of an electronic device, and it supports an information society. To realize the Internet of Things (IoT) society, the miniature, an enormous amount of the sensor is required, and these are usually produced by the MEMS.

One of a field of the MEMS process, the mechanical field is researched because it can form a miniature high aspect ratio pattern. Miniature MEMS actuators are researched for miniature mechanical systems [2–5]. Moreover, attention is paid to microrobots that have miniature silicon mechanical components. These robots have miniature body structure and miniature actuator [6–9]. The miniature actuators and the miniature robot can be used for the medical field. The miniature structure can work in the narrow space such as inside of a human body. For example, an endoscope microrobot has been researched [10].

The MEMS can realize the development of the information society and the medical field. However, a miniature power source is required for the electronic device such as the sensor, the actuator and the microrobot. Conventionally, a lithium-ion-secondary battery is used as the small- and high-power density source, but it is too large for these electronic devices. Moreover, the power density of the lithium-ion-secondary battery is approaching to the theoretical limit. Therefore, the MEMS power generators have been studied for miniature power supply system. To keep a micro scale, many researchers use a piezoelectric vibration power generator [11, 12]. It uses only a material characteristic without complex mechanical structure. However, these generators harvest the force to move the device by the environmental vibration, and then, its power is too small to be used for main power source.

On the other hand, ultra-micro gas turbine (UMGT) that used an electrostatic type was reported by the MIT group [13]. It was a remarkable generator because of its extremely high energy density in small size. The advantage of the electrostatic-type power generator is that the components are based on planar structure, and it is easy to fabricate by the MEMS process. A lot of studies on the electrostatic-type MEMS generator have been reported [14]. However, it shows charge saturation and high internal impedance; as a result, an output current of the electrostatic-type generator becomes small. For this reason, an electromagnetic induction type that is usually used a commercial size generator has been studied in the MEMS generator. The electromagnetic induction type shows low output impedance and high output power.

The conventional electromagnetic induction-type generator has a magnet, moving part such as the turbine structure, and a magnetic circuit including a magnetic core. The winding wire magnetic circuit forms a three-dimensional coil structure. In the MEMS process, the miniature moving part can realize, but it is difficult to form the three-dimensional structure coil by using the MEMS process. Therefore, the planer structures such as a spiral, a meandering or equivalent shape are employed for the electromagnetic induction-type MEMS generator. The complex three-phase coil pattern made from a copper conductor that was arranged on a plane substrate has reached milliwatt to watt class [15, 16]. However,

http://dx.doi.org/10.5772/intechopen.74830

the planar structure coil requires the large area if the turn number increases because the conductor patterns extend parallel on the surface. Also, it is difficult to use the magnetic material. Therefore, to catch the magnetic flux, long length coil is required. As a result, it shows high internal resistance and small output power. In order to realize the miniature electromagnetic induction-type generator, the miniature three-dimensional structure coil that has the magnetic core is required.

The multilayer ceramic technology is suitable for forming the miniature three-dimensional structure coil. This technology is the fabrication technology of a miniature electronic component like a multilayer ceramic inductor. It can form a three-dimensional circuit pattern inside a ceramic material. A ferrite ceramic material shows excellent magnetic property, and the multilayer ceramic technology will realize the miniature monolithic structure that has the three-dimensional structure coil and the magnetic core.

In this chapter, the miniature electromagnetic induction-type air turbine generator is proposed and developed. The proposed generator is combined with the miniature MEMS air turbine structure and the miniature multilayer ceramic magnetic circuit. To achieve milliwatt-level output power, it is required that high rotational speed of the rotor. Therefore, the air turbine is discussed optimization of a rotating structure. The various complex structure multilayer ceramic magnetic circuits are proposed. The proposed magnetic circuits are discussed and optimized the shape to catch the magnetic flux. Moreover, the fabricated air turbine generator demonstrates the rotational motion and power generation.

2. Design and concept of MEMS air turbine generator

2.1. Electromagnetic induction-type MEMS air turbine generator

The electromagnetic induction type is employed for developed MEMS air turbine generators. Proposed MEMS air turbine generators are combined with the MEMS mechanical parts and the ceramic electronic part. In the MEMS air turbine structure, a magnet is connected to the rotor. The rotor shows a rotational motion by the inletting fluid. This motion occurs the electromagnetic induction revolving-field.

The design concept of the air turbine is the high-speed rotational motion. The rotational structure at a bearing system and a rotor blade form are compared. In the bearing system, the fluid dynamic bearing system and a miniature ball bearing structure are discussed. The rotor blade forms influence the rotational motion. In this chapter, a flat-type rotor blade and a rim-type rotor blade are compared. Therefore, three types of air turbine structures are designed and fabricated. The design concepts of the ceramic magnetic circuit are a miniature three-dimensional structure coil and the introduction of the magnetic flux. The magnetic material designs of the circuit are analyzed, and these are compared. Moreover, the arrangement of the magnetic circuit is an important factor to the miniature electromagnetic induction-type generator. The arrangement of the magnetic circuit is discussed as the generator that combined with the air turbine and the magnetic circuit.

2.2. Mechanical parts of generator

The mechanical parts of the generator are the air turbine structure. These are made from a miniature silicon parts, and the miniature structure parts are fabricated by the MEMS process. To achieve the high-speed rotational motion, two types of bearing system such as a fluid-dynamic bearing system and a miniature ball bearing system are designed. The one of the bearing system, a fluid-dynamic bearing system is employed. In the miniature structure, the friction force influence to the rotational motion. Therefore, a contactless-type miniature bearing system is advantaged for the miniature silicon air turbine. However, it is difficult to rotate with stability by this method. Moreover, design of the air turbine will be complex because it requires flow passages to rotating and floating.

Another one is the miniature ball bearing. It made from a mechanical process, and it can suppress an eccentric motion of the rotor because the ball bearing holds the rotor directly. The rotor and the magnet are held a shaft through the ball bearing structure. It requires the initial torque to achieve the rotational motion, but it is desired a stable rotational motion and the simple structural design. By using the miniature ball bearing, the rotational part and the magnet part can separate.

The MEMS air turbine designs are shown in **Figures 1** and **2**. **Figure 1** shows the flat-type rotor blade and the fluid dynamic bearing system air turbine. Image (a) and (b) of the **Figure 2** employs the miniature ball bearing structure for the bearing system. Image (a) uses the flat-type rotor blade air turbine and (b) uses the rim-type rotor blade air turbine, respectively.

The air turbine parts of **Figure 1** are seven silicon structural layers and the rotor that has the magnet. The upper layers form the air passage structure. Through this passage, air is passed to the stator and it generates the rotational motion of the rotor. The ring-shaped magnet is

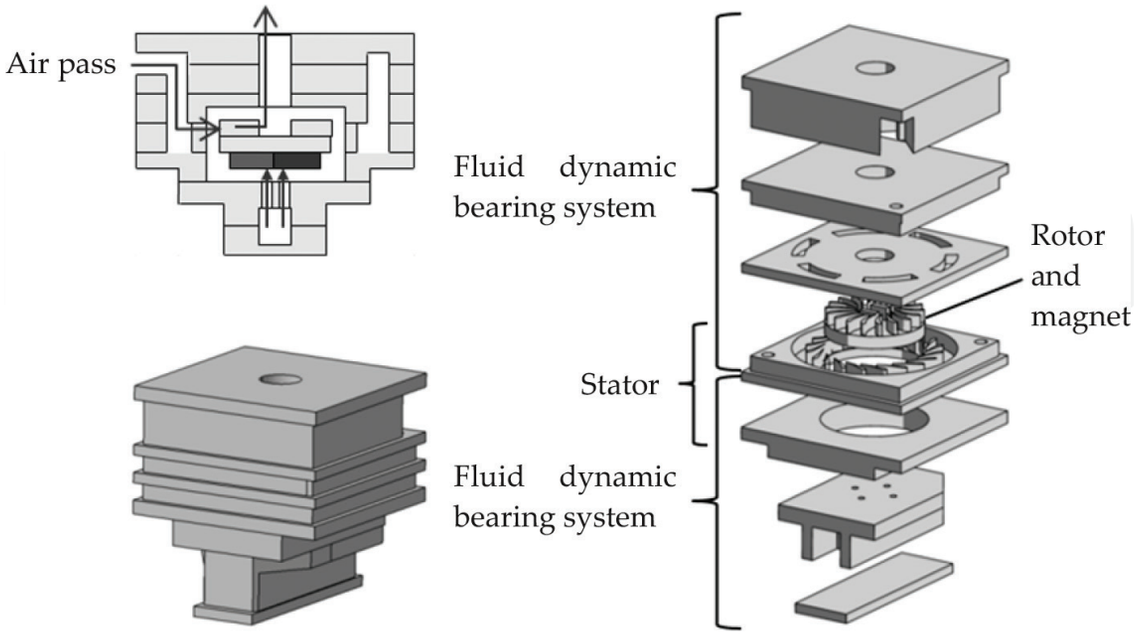

Figure 1. Design of MEMS air turbine structure that has flat-type rotor blade and fluid dynamic bearing system.

attached to the rotor and placed in a center of the stator. The lower layers form the passage for the fluid dynamic bearing system. The shape of the lower layers that form the fluid dynamic bearing system is bump structure. This structure realizes a short distance between the magnet and the magnetic circuit. However, the gap between the magnet and the magnetic circuit is more than 800 μm. The designed flat-type rotor has the plate structure under the rotor blade. The plate receives the air through the levitation passage, and then, the air is released from an outlet. The rotational air through the stator is introduced to the center of the rotor, and then, the air passed the same outlet. The designed dimensions of the air turbine are 3.0, 3.0 and 3.0 mm, length, width and height, respectively.

Designed turbines in **Figure 2** have a difference at the arrangement of the miniature ball bearing. The flat-type rotor blade (a) has one miniature ball bearing inside the air turbine structure. The air turbine parts are made from 11 silicon layers and 3 silicon rotor parts. The compressed air flows from side inlet, and the down flow air passes to the stator and the rotor. The released air passes a top outlet. The dimensions of the miniature ball bearing are 2.0 mm (outer diameter), 0.6 mm (inner diameter) and 0.8 mm (height), respectively. It is made by a martensitic stainless steel. The rotor is putted on the ball bearing. The magnet is arranged under the bearing structure. Then, these are connected to the ball bearing through the shaft. The diameter of the shaft is 0.593 mm, the material is cemented carbide. The flat-type rotor shape is the same design with the fluid dynamic bearing system air turbine. The magnet and a magnetic yoke are combined to suppress a leaked magnetic flux. The ring-shaped magnet is neodymium magnet 2-pole radial direction. Its dimensions are outer diameter 3.0 mm, inner diameter 1.0 mm and height 0.5 mm, respectively. The ring-shaped magnet yoke is formed by a silicon steel sheet. The dimensions of the magnet yoke are outer diameter 3.0 mm, inner diameter 1.0 and height 0.38 mm, respectively. The size of the designed air turbine is 5.20 mm, 5.20 and 4.50 mm, length, width and height, respectively.

In the image (b) of **Figure 2**, two ball bearings are used for holding the rotor and the magnet. The bearings are placed above and below the rim-type rotor. The air turbine structure is constructed by seven silicon layers, rotor and magnet supporting part. The air passage for rotational motion of the rotor is formed around the rim-type rotor, and the compressed air flows from side inlet to side outlet. Thickness of the rotor blade is 750 μm, and the rotor blades are formed on the side wall of the rotor. The dimensions of the rim type are 5.20, 5.20, 4.60 mm length, width and height, respectively. The ball bearing-type air turbine can separate the rotor and the magnet because these are held by the shaft. Therefore, the gap between the magnet and the magnetic circuit is shorter than the fluid dynamic bearing-type air turbine. The gap dimension of the design (a) is 220 μm and (b) is gapless design.

The fine pattern of the rotor and each layer were fabricated by the photolithography process. In this process, the miniature components were fabricated from single crystal silicon wafer. Each silicon wafer for the parts was washed, deposited with an aluminum layer by physical vapor deposition, and coated with a photoresist. The designed pattern was exposed to the resist layer and developed by soaking in the developer. The aluminum layer on the specimen was then chemically etched, leaving an imprint of the designed pattern. The patterned wafer was dry etched by high aspect ratio inductively coupled plasma etching combined with

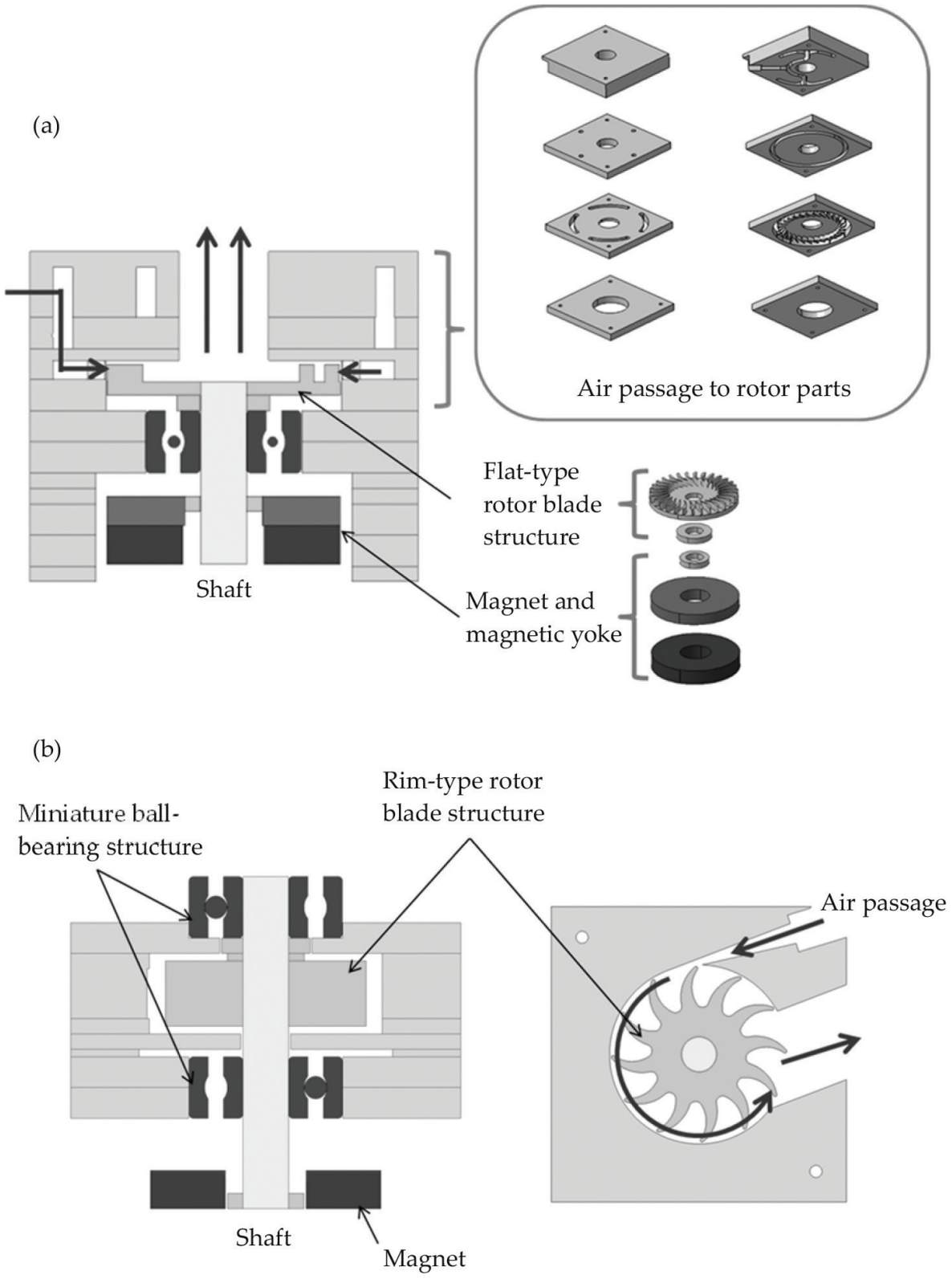

Figure 2. Design of MEMS air turbine structures (a) flat-type rotor blade and miniature ball bearing and (b) rim-type rotor blade and miniature ball bearing.

http://dx.doi.org/10.5772/intechopen.74830

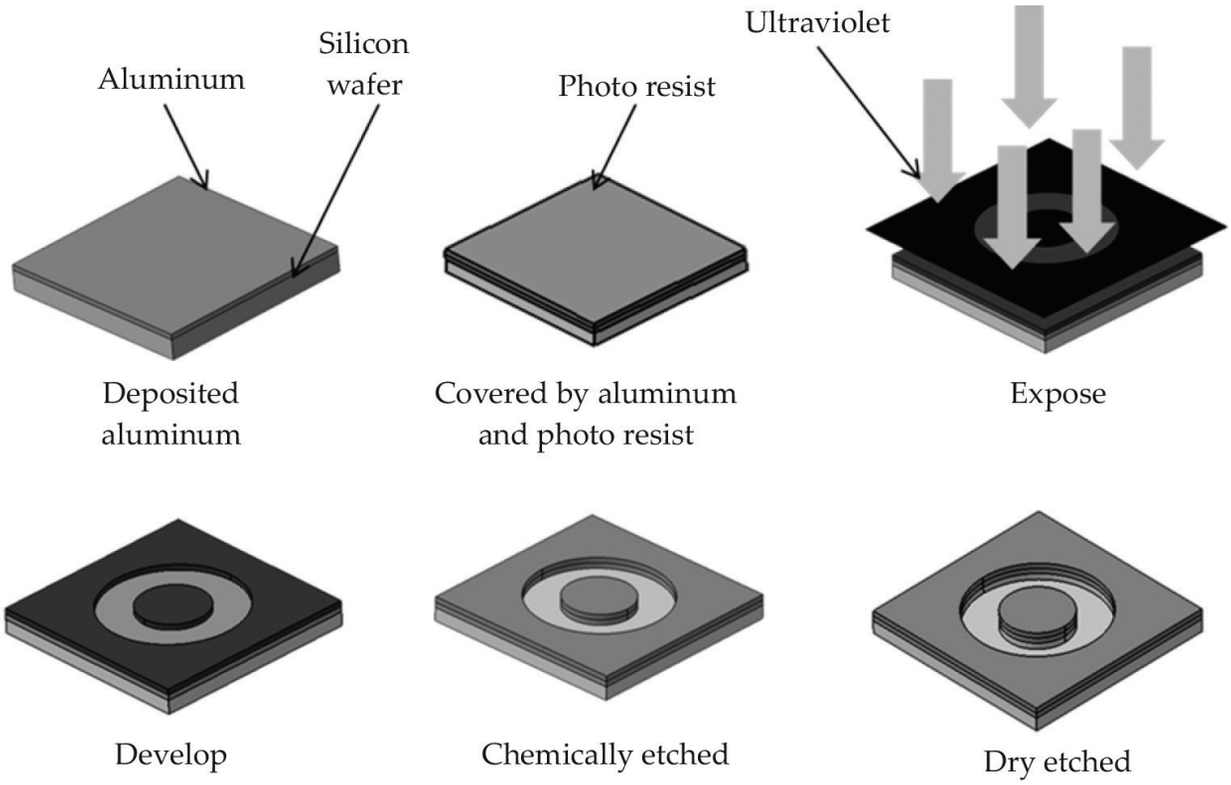

Figure 3. Fabrication process for miniature components of designed MEMS air turbine.

a Bosch process [1]. The parts were achieved after removing the aluminum and washing. Through these processes, the silicon structural components were fabricated. The obtained components were assembled by hand and alignment pin. **Figure 3** shows the schematic illustration of the fabrication process.

2.3. Electronic parts of generator

The electronic part for the electromagnetic induction-type MEMS air turbine generator is the magnetic circuit. To achieve the miniature generator, the miniature magnetic circuit that has a three-dimensional structure coil and a magnetic core for introducing a magnetic flux is required. Moreover, low internal resistance is an important factor to achieve high output power. Therefore, the three-dimensional coil pattern is required. The multilayer ceramic technology is used for the magnetic circuit. Optimization of the magnetic circuit design and the fabrication process are explained.

Designs and analyzed results of the magnetic circuit for the miniature generators are shown in **Figures 4** and **5**. **Figure 4** shows designs for the fluid dynamic bearing system-type air turbine generator. The shape of (a) is a step-wise shape, and (b) is a horseshoe-shaped structure. These magnetic circuits have two-pole coil structures. Each pole has 12 turn coil structure, and they are connected at the connecting layer. Therefore, the designed magnetic circuits have 24

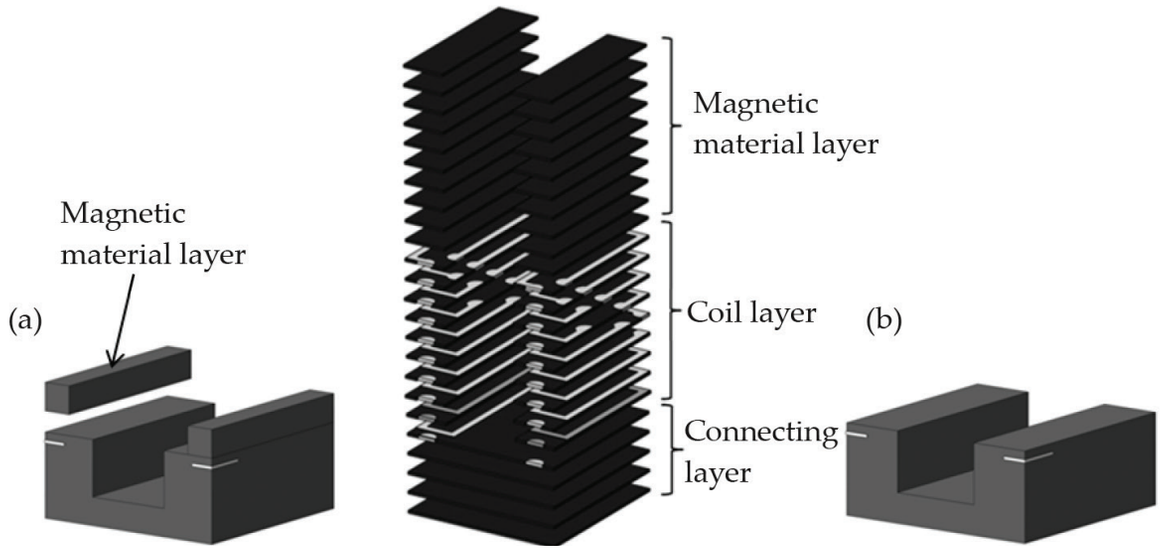

Figure 4. Design of the magnetic circuits for fluid dynamic bearing system generator: (a) step-wise shape and (b) horseshoe shape.

turn coil. The horseshoe-shaped circuit has only the coil layer and the connecting layer, and the step-wise shape circuit has the magnetic material layer. When the magnetic circuit and the air turbine are combined, the magnet inside the air turbine is placed between the magnetic material layers. The magnetic flux loss is compared between the magnetic circuits. The results are shown in **Figure 5**. The magnetic flux is introducing from the magnet to magnetic circuit in (a). On the other hand, (b) shows the magnetic flux loss more than (a). In the both structures, the dimensions are 3.5 and 3.5 mm, length and width, respectively. The heights are 2.0 mm in the step-wise shape and 1.2 mm in the horseshoe shape.

The output powers of these designs magnetic circuit are compared. In this evaluation, a spindle machine is used for power evaluations.

Figure 6 shows the around-type magnetic circuit. It is used for the miniature ball bearing-type air turbine generator. Designed magnetic circuit is constructed by four pieces. The coil layers

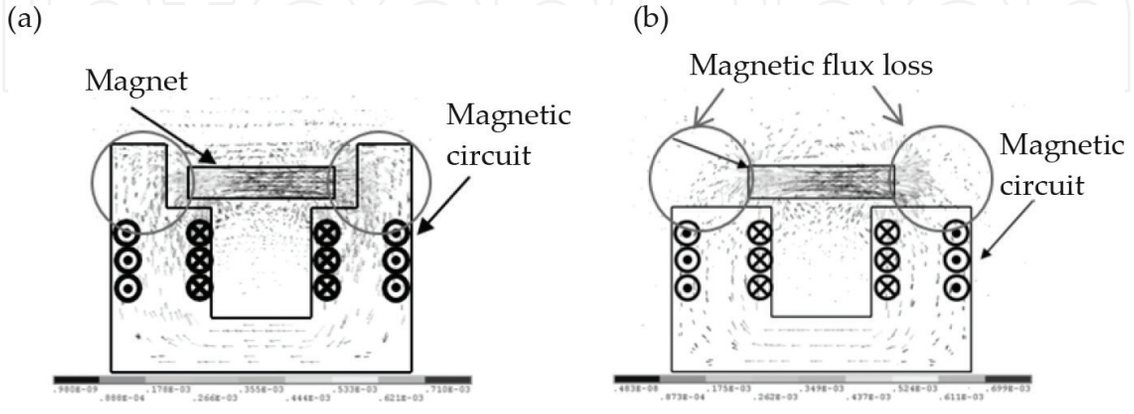

Figure 5. Analyzed results of the magnetic circuits: (a) step-wise shape and (b) horseshoe shape.

http://dx.doi.org/10.5772/intechopen.74830

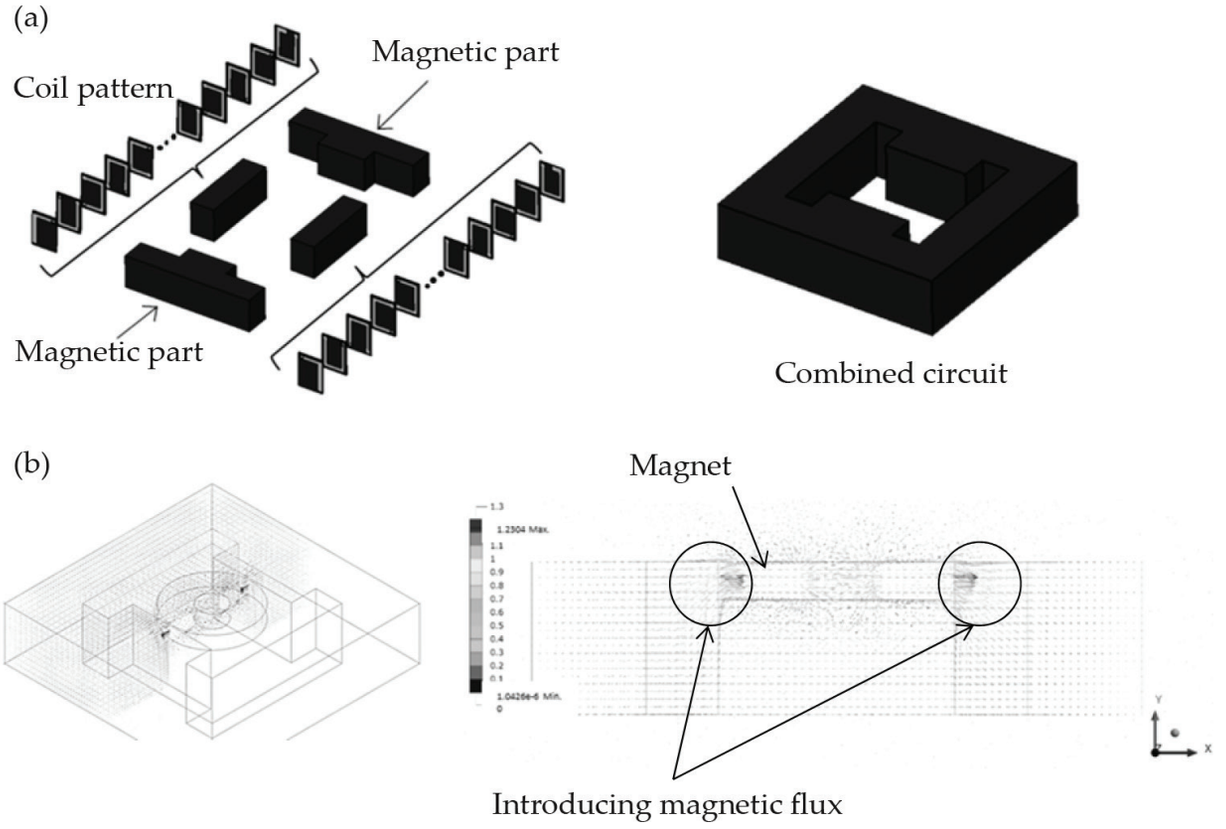

Figure 6. Design of around-type magnetic circuit for ball bearing-type air turbine (a) schematic illustration of circuit design, (b) analyzed result.

are arranged in side parts, and these have 50 turns each other. The total number of coil turns is 100 turns; these are bonded with the magnetic parts for introducing the magnetic flux. By this process, the closed magnetic circuit is obtained. The magnetic parts are introducing the magnetic flux from the magnet. In **Figure 6**, the analyzed result is shown in (b). By this result, the magnetic flux through the magnetic parts were observed. Dimensions of the designed circuit are 7.40, 8.50, 2.40 mm, length, width and height, respectively.

The magnetic ceramic material is low-temperature co-fired Ni-Cu-Zn ferrite with the permeability of 900. The compositional ratio is 49.2 Fe_2O_3–8.8 NiO-10 CuO-32ZnO. The Ni-Cu-Zn ferrite can be fired at around 900°C. Therefore, it is possible to use the low-resistance silver conductive material.

The fabrication process for the miniature magnetic circuits is the green sheet process, that is, the multilayer ceramic technology. In this process, the ceramic slurry was made for forming a sheet structure. This sheet is called the green sheet. The slurry in our fabrication was made of the mixture of the ferrite ceramic powder, binder, dispersing agent, plasticizer and organic materials. The through hole for connecting the under layer was machined, and then the coil pattern was printed on the ferrite green sheet by the screen printing technology. The material of the coil pattern was silver paste as a conductor paste. The multiple sheets were stacked, and the specimen was diced into the designed part. By using the magnetic ceramic for the green

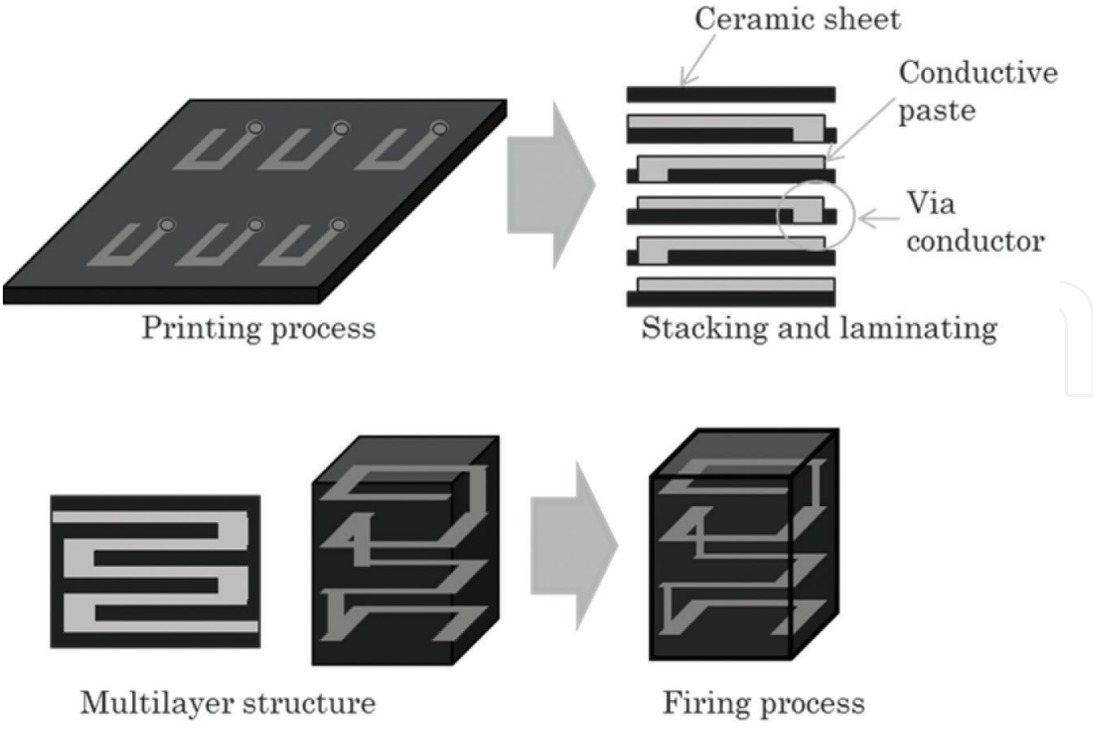

Figure 7. Schematic illustration of fabrication process for multilayer ceramic coil pattern.

sheet, the magnetic core is formed simultaneously. Through this process, the obtained specimen was a planar structure that had the miniature coil pattern inside the magnetic ceramic. **Figure 7** shows the schematic illustration of the fabrication process for the multilayer ceramic coil pattern.

In order to combine the MEMS air turbine, more complicated structure is required. Each part was combined for the design structure. After that, the specimen was fired in the electric furnace. In the around-type coil, the pieces were firing. After that, the pieces were combined because a shrinkage process deforms the ceramic coil. Through these processes, the objective structure was completed. A schematic illustration of the combined process for the complex structure coil is shown in **Figure 8**.

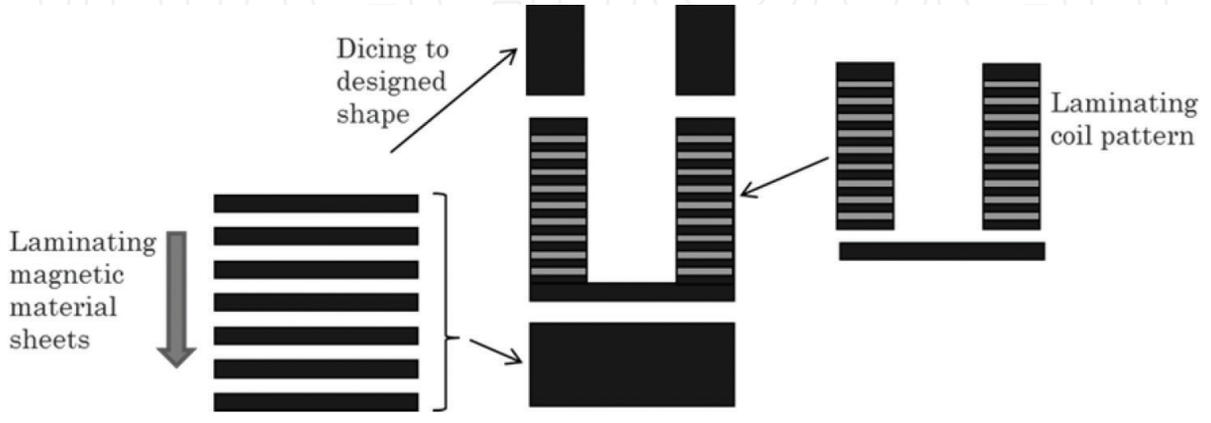

Figure 8. Schematic illustration of the combined process for the complex structure coil.

http://dx.doi.org/10.5772/intechopen.74830

2.4. Experimental procedure

The combined MEMS generator was evaluated on the output power. The compressed nitrogen gas was injected to the MEMS generator. The rotational speed and the output voltage were measured. Load resistances were connected to the ceramic magnetic circuit. The output waveform was measured by an oscilloscope.

3. Results and discussion

The fabricated MEMS air turbines and the multilayer ceramic magnetic circuits were evaluated. The combined electromagnetic induction-type MEMS air turbines were evaluated on the power generation.

3.1. Fluid dynamic bearing system air turbine generator

The fabricated components of the fluid dynamic bearing system air turbine and the assembled MEMS air turbine are shown in **Figure 9**. Designed dimensions and the measured dimensions are shown in **Table 1**. As a result, it is found that the error was less than 5 μm.

Figure 10 shows the fabricated multilayer ceramic magnetic circuits. The dimensions of the step-wise shape multilayer ceramic circuit were 3.40, 3.47 and 1.88 mm, length, width and height, respectively. Inductance and DC resistance were 5.35 μH and 0.53 Ω. The dimensions of the horseshoe shape circuit were 3.25, 3.49 and 1.34 mm, length, width and height, respectively. Inductance and DC resistance were 5.85 μH and 0.94 Ω.

The result of the power generation experiment by the spindle machine is shown in **Table 2**. The load resistance of 1 Ω was connected to both magnetic circuits. The rotational speed of the spindle machine was 300,000 rpm. By the results, the maximum output power of the

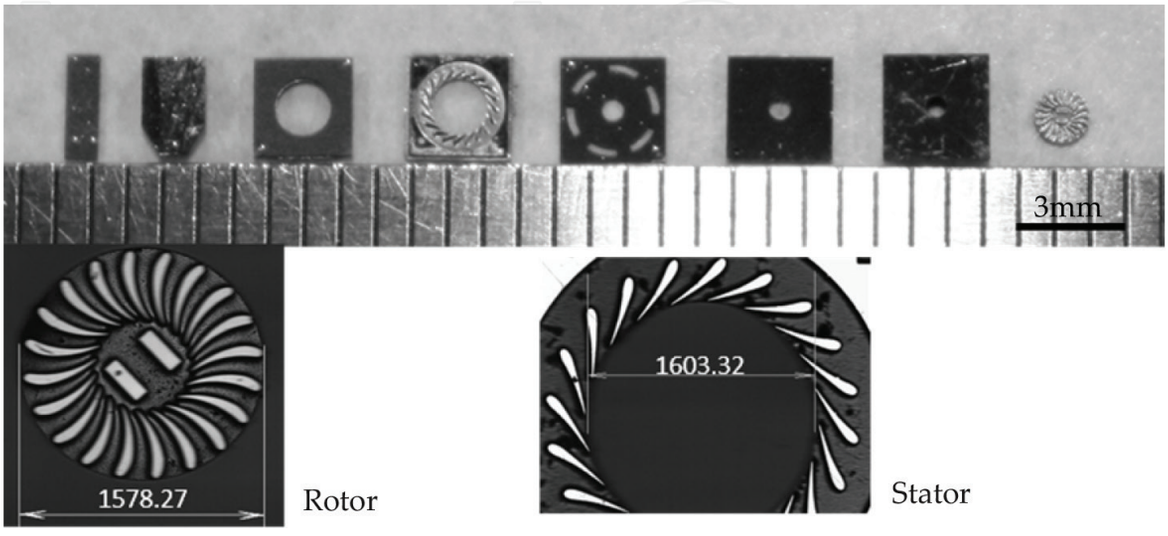

Figure 9. Fabricated fluid dynamic bearing system air turbine components.

	Design dimension (μm)	Measured dimension (μm)
Rotor diameter	1580	1578.27
Stator diameter	1600	1603.32

Table 1. Dimensions of the MEMS air turbine components.

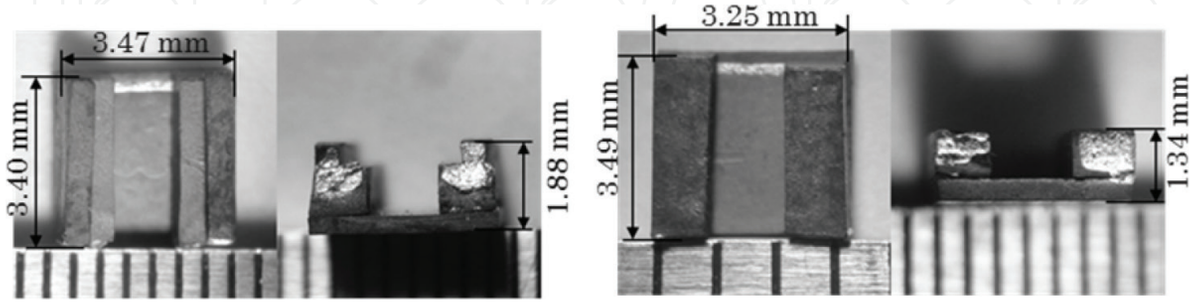

Figure 10. Fabricated multilayer ceramic magnetic circuit: (a) step-wise shape and (b) horseshoe shape.

step-wise shape was 1.47 mVA, and the output power of the horseshoe shape was 0.72 mVA. The step-wise shape magnetic circuit showed the larger output power than the horseshoe shape magnetic circuit. It is agreed from the result of the analyses. Therefore, it is found that the magnetic material surrounding the magnet improved the output power.

The fabricated MEMS air turbine and the multilayer ceramic magnetic circuit were combined. **Figure 11** shows the MEMS air turbine generator and its output voltage waveform. The step-wise shape magnetic circuit that shows the internal resistance of 1.05 Ω was used. The dimensions of the MEMS air turbine generator were 3.50, 3.47 and 3.86 mm, length, width and height, respectively. The maximum rotational speed was 30,000 rpm on the condition of 0.28 MPa. The load resistance of 1 Ω was connected to the output of the magnetic circuit. The maximum output voltage and the output power of the generator were 1.32 mV and 1.74 μVA, respectively. In the rotational motion, the fluid dynamic bearing system air turbine rotor showed the eccentric motion.

3.2. Miniature ball bearing air turbine generator

The fabricated components and the assembled structure of the flat-type rotor blade air turbine are shown in **Figure 12**. Dimensions of the structure were 5.23, 5.20, 4.51 mm length, width and height, respectively. **Figure 13** shows the fabricated components and the assembled struc-

	Output voltage [mV]	Output power [mVA]
Step-wise shape	26.8	1.47
Horseshoe shape	38.4	0.72

Table 2. Power generation results of fabricated magnetic circuit using spindle machine.

http://dx.doi.org/10.5772/intechopen.74830

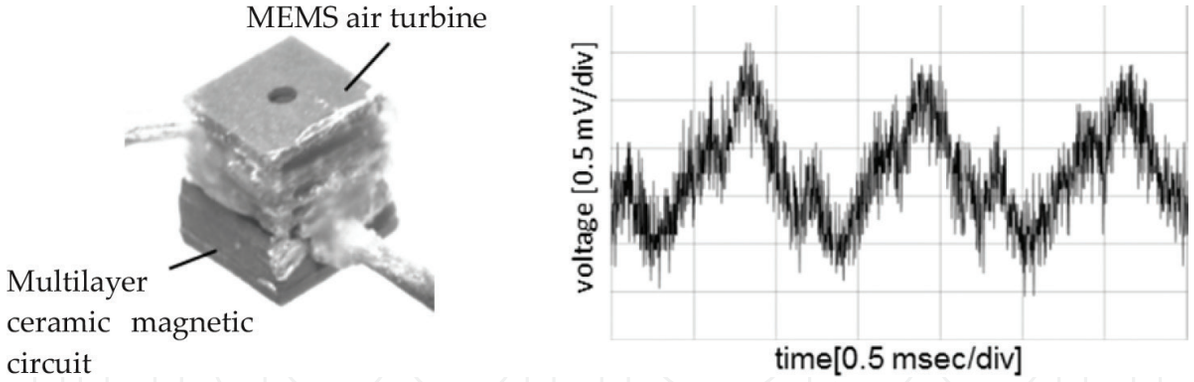

Figure 11. Fabricated MEMS air turbine generator and its output voltage waveform.

ture of the rim-type rotor blade air turbine. Dimensions were 5.24, 5.37, 4.64 mm length, width and height, respectively. These fabricated MEMS air turbine were evaluated on the rotational speed. The rotational speed was measured by a hall sensor. The comparison of the rotational speed is shown in **Figure 14**. The flow rate changed from 0 to 1.0 l/min. at pressure of 0.3 MPa. Experimental result shows that the rim-type system had a superior potential to the planar type. The flux change dependents the rotational speed because the magnet attached to the rotor. The high rotational speed air turbine is advantage for high output power. Therefore, to achieve high output power, the rim-type air turbine was employed the generator.

The fabricated multilayer ceramic magnetic circuit was shown in **Figure 15**. Dimensions of the circuit were 7.40, 8.47, 2.36 mm, length, width and height, respectively. The measured DC resistance was 2 Ω.

The fabricated rim-type air turbine and the magnetic circuit were combined. **Figure 16** shows the combined electromagnetic induction-type MEMS air turbine generator. Dimensions of the generator were 7.40, 8.47, 5.82 mm, length, width and height, respectively. When the maximum

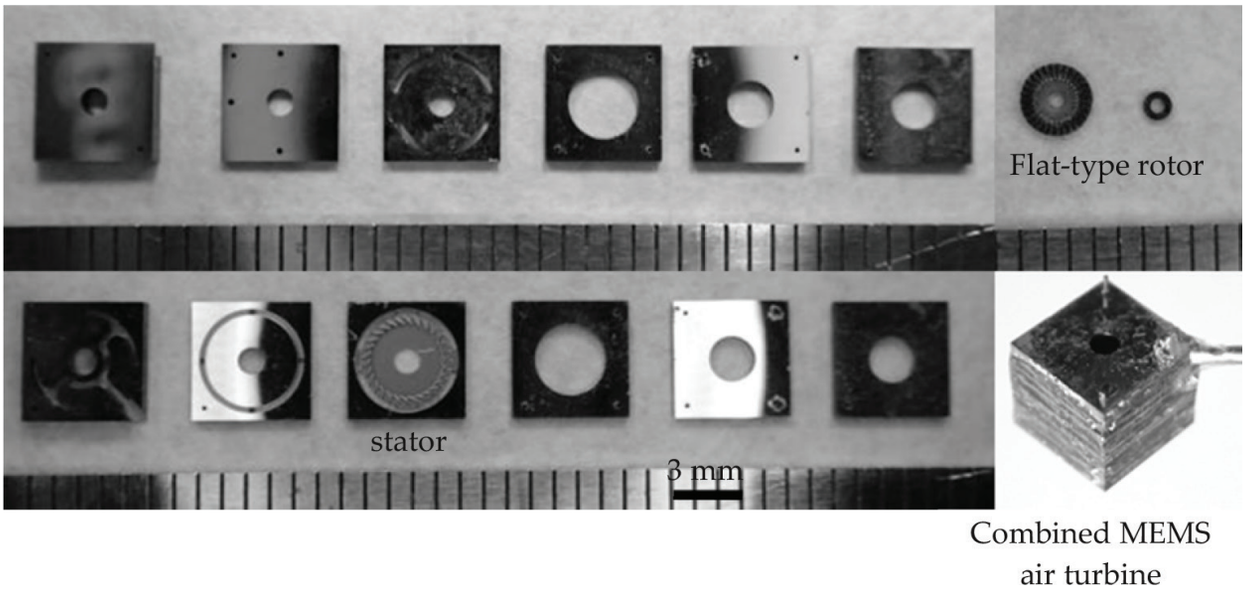

Figure 12. Fabricated components and assembled structure of flat-type rotor blade air turbine.

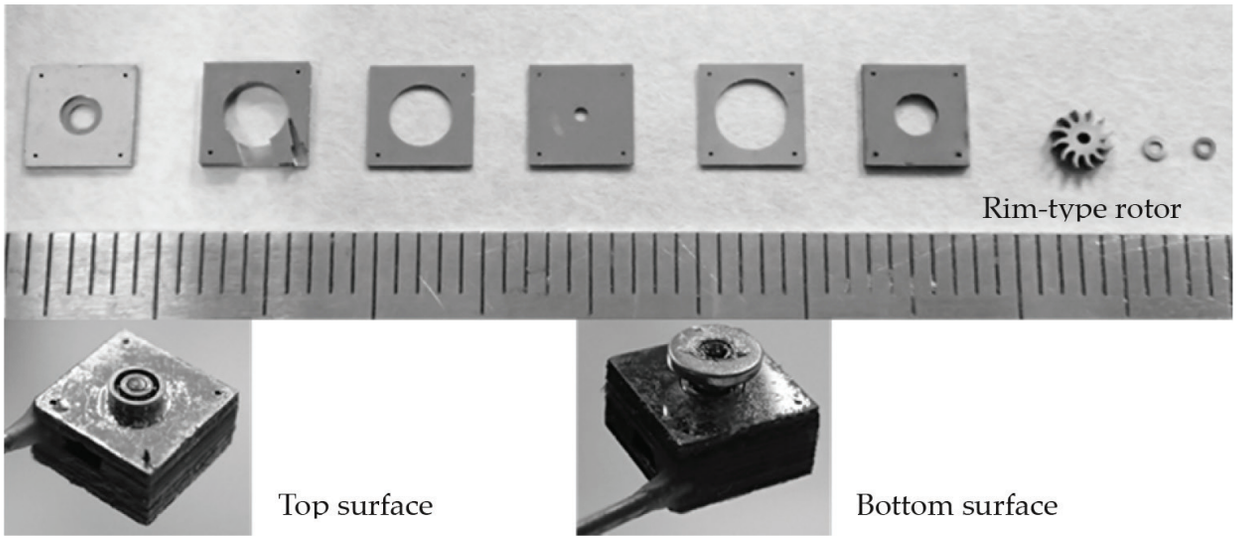

Figure 13. Fabricated components and assembled structure of rim-type rotor blade air turbine.

rotational speed was 290,135 rpm, the inlet flow was 2.4 l/min and the pressure was 0.3 MPa. The output voltage and the output power at each load resistance are shown in **Figure 16**. The maximum output power was 2.41 mVA when the load resistance was 8 Ω, and the output voltage of 139 mV was shown. The output waveform at the load resistances was 8 and 1 kΩ, as shown in **Figure 17**.

The output voltage $V = R_L I$ is given by the following equation: (1) when the load resistance R_L is connected to the generator and the current I flows through the circuit. In this equation, it is necessary to consider the influence of the voltage drops by the self-inductance L and the internal resistance r of the connected magnetic circuit.

$$V = R_L I = N\, d\varphi/dt - i\omega LI - rI \tag{1}$$

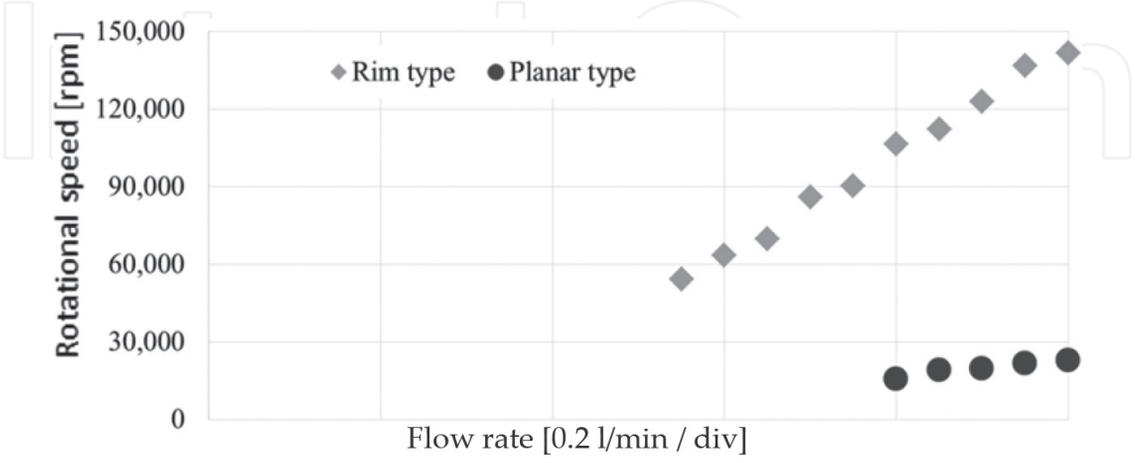

Figure 14. Comparison of rotational speed.

http://dx.doi.org/10.5772/intechopen.74830

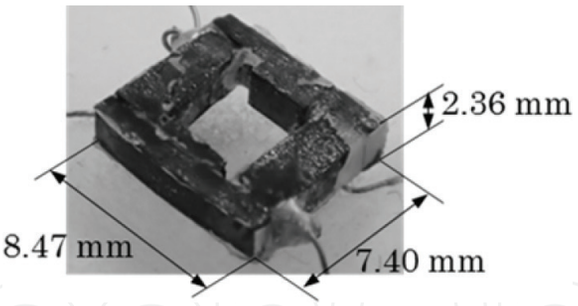

Figure 15. Fabricated multilayer ceramic magnetic circuit.

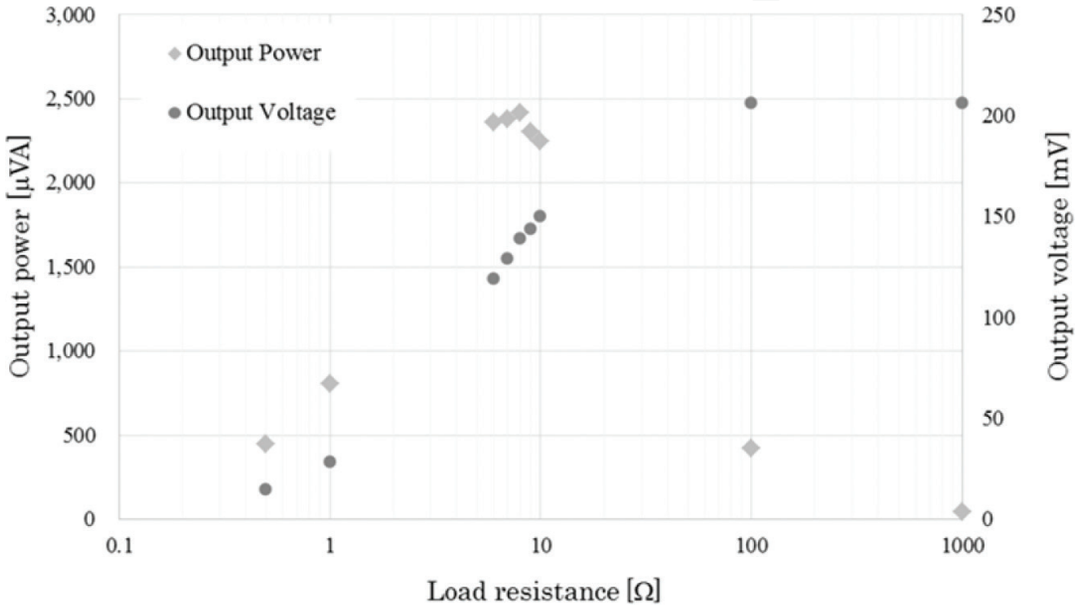

Figure 16. Output voltage and output power at each load resistance.

The magnetic flux passing the magnetic circuit is φ. N is the turn number of coil. L is the measured value at the equivalent frequency of 290,135 rpm (impedance analyzer: Agilent 4294A), and it was 241 μH. When the R_L was 1 kΩ, the voltage drop due to self-inductance and the internal resistance become small because the current carrying the circuit is sufficiently small. Therefore, the output voltage is approximated by $d\varphi/dt$. The surface magnetic flux density of the permanent magnet and the magnitude of the magnetic flux on the magnet surface are 0.159 T and 0.375 μWb, respectively. Theoretical value if the all flux enters in the circuit, the output voltage was calculated to be 570 mV. Compared with the output voltage that connected 1 kΩ, 36% of the maximum magnetic flux contributes to the actual power generation. On the other hand, when R_L of 8 Ω was connected, the reactance of ωL is calculated 7.3 Ω. As a result, values of ωL and r are close to R_L, and their influence appears. The absolute value of the output voltage is estimated as Eq. (2).

$$| V | = \left(N\, d\varphi/dt\, R_L\right)/\left[\left(R_L + r\right)^2 + \omega^2 L^2\right]^{1/2} \quad (2)$$

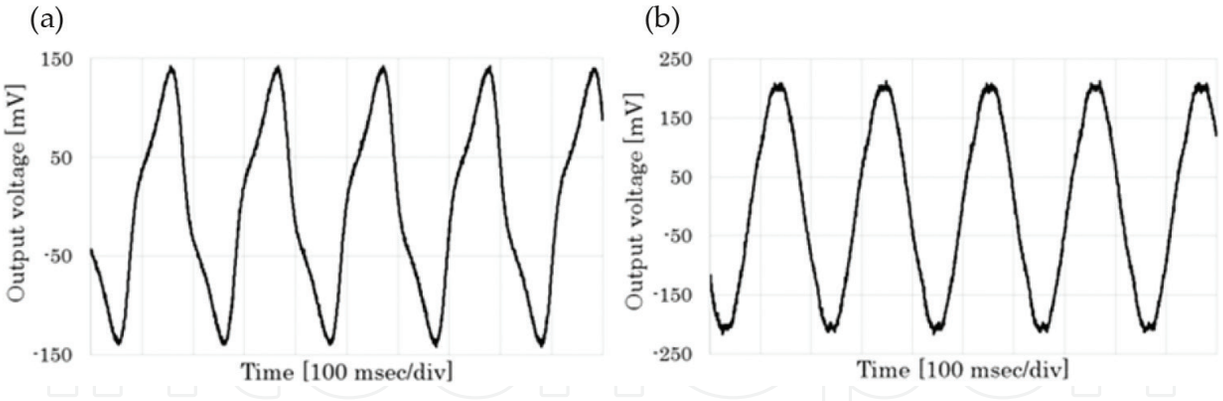

Figure 17. Output waveform at the load resistances were (a) 8 Ω and (b) 1 kΩ.

The calculated result of Eq. (2), |V| becomes 367 mV. If the contribution rate 36 % of the magnetic flux to this result, |V| become 132.12 mV. It almost coincides with output voltage at 8 ohm (**Figure 17(a)**).

In the electromagnetic induction type, the magnetic circuit occurs a braking torque to the permanent magnet. However, the rotational speed of **Figure 17(a)** and **(b)** shows almost equal. Therefore, the braking torque by current is sufficiently small in this turbine structure. The magnetic flux density from the magnetic circuit can be calculated at Eq. (3).

$$B = \mu_0 \mu_r NI \tag{3}$$

The vacuum permeability and the ferrite relative permeability are expressed in μ_0 and μ_r. As a result, B is calculated as 1.96 mT. The maximum braking torque occurs when the magnetization of the permanent magnet and the magnetic flux density of the magnetic circuit cross perpendicular. If all the magnetic flux contributes, the braking torque is 42.9 pNm. This value is considered as sufficiently small value.

4. Conclusions

The electromagnetic induction-type MEMS air turbine generator was proposed. In this chapter, three types of MEMS air turbine generators that included the different bearing systems, shape of the rotor blades and shape of the magnetic circuits were discussed to achieve the high output power. In the MEMS air turbine, the purpose was achieving high-speed rotational motion. The magnetic circuit required the miniature structure that had the three-dimensional coil, magnetic core and magnetic flux introduction design. Therefore, the multilayer ceramic technology and the ferrite ceramic were used. One of the developed air turbines employed the fluid dynamic bearing system and flat-type rotor. In the miniature structure, the contactless-type miniature bearing system is advantaged because the friction force is impact issue. Moreover, two types of magnetic circuits for the fluid dynamic bearing turbine generator were compared with the magnetic flux loss. By the power generation experiment, the stepwise shape circuit that had the magnetic material introducing the magnetic flux from the magnet was suitable to the generator. The fabricated MEMS air turbine generator showed the

output power of 1.74 μVA, when the rotational speed was 30,000 rpm, the output voltage was 1.32 mV and the load resistance of 1 Ω was connected. However, it showed eccentric motion because it was not supported by structurally. Therefore, another one of the air turbines used the miniature ball bearing system. The developed ball bearing air turbines were compared with the rotational speed between the different rotor blades. As a result, the rim-type rotor blade showed high rotational speed than the flat-type rotor. Moreover, the ball bearing-type air turbine could separate the magnet from the rotor. Therefore, the short distance between the magnet and the magnetic circuit was realized. The shape of the magnetic circuit was around type that had the magnetic flux induction parts. To evaluate the power generation, the rim-type air turbine and the around-type multilayer ceramic magnetic circuit were combined. The maximum rotational speed was 290,135 rpm. The output power of fabricated MEMS air turbine generator was 2.41 mVA when the load resistance was 8 Ω and the output voltage of 139 mV was shown. By these results, the milliwatt-level MEMS air turbine generator was realized by the high-speed rotational motion structure that had the rim-type rotor blade and the miniature ball bearing system, and by introduction of the magnetic flux.

Acknowledgements

The sample of this study was fabricated by the facility at the Research Center for Micro Functional Devices, Nihon University. Part of this study was supported by the CST research project of Nihon University and by JSPS KAKENHI (16 K18055).

Author details

Minami Kaneko*, Ken Saito and Fumio Uchikoba

*Address all correspondence to: takato@eme.cst.nihon-u.ac.jp

Department of Precision Machinery Engineering, College of Science and Technology, Nihon University, Chiba, Japan

References

[1] Bhardwaj Jy K, Ashraf H. Advanced silicon etching using high-density plasmas. In: Proceedings of the SPIE Micromachining and Microfabrication Process Technology; 19 September 1995; Austin, TX, United States. pp. 224-233

[2] Long-Sheng F, Yu-Chong T, Muller RS. IC-processed electrostatic micro-motors. In: Proceedings of the Int. Electron Devices Meeting (IEDM '88). Technical Digest; 11-14 December 1988; San Francisco, CA, United States. pp. 666-669

[3] Zhang W, Zou Y, Lin T, Chau FS, Zhou G. Development of miniature camera module integrated with solid tunable lens driven by MEMS-thermal actuator. Journal of Microelectromechanical Systems. 2017;**26**:84-94. DOI: 10.1109/JMEMS.2016.2602382

[4] Berka MJ, Yadid-Pecht O, Mintchev MP, Wang GMEMS. Actuator for splinter-like skin penetration in glucose-sensing applications: Design and demonstration. In: Proceedings of 2016 IEEE SENSORS; 30 October-3 November 2016. Orlando, FL, USA: IEEE; 2017. DOI: 10.1109/ICSENS.2016.7808549

[5] Junagal K, Meena RS. Design and simulation of microstage having PZT MEMS actuator for 3D movement. In: Proceedings of International Conference on Advances in Computing, Communications and Informatics (ICACCI); 21-24 September; Jaipur, India. DOI: 10.1109/ICACCI.2016.7732375

[6] Donald BR, Levey CG, McGray CG, Paprotny I, Rus D. An untethered, electrostatic, globally controllable MEMS micro-robot. Journal of Microelectromechanical Systems. 2006;**15**(1):15. DOI: 10.1109/JMEMS.2005.863697

[7] Vogtmann D, Pierre St. R, Bergbreiter S. A 25 mg magnetically actuated microrobot walking at > 5 body lengths/sec. In: Proceedings of 2017 IEEE 30th International Conference on Micro Electro Mechanical Systems (MEMS); 22-26 January 2017; Las Vegas, NV, USA. pp. 179-182

[8] Murthy R, Stephanou HE, Popa DO. AFAM: An articulated four axes microrobot for nanoscale applications. IEEE Transactions on Automation Science and Engineering. 2013;**10**:276-284

[9] Elbuken C, Khamesee MB, Yavuz M. Design and implementation of a micromanipulation system using a magnetically levitated MEMS robot. IEEE/ASME Transactions on Mechatronics. 2009;**14**:434-445

[10] Yan G, Ye D, Zan P, Wang K, Ma G. Micro-robot for endoscope based on wireless power transfer. In: Proceedings of International Conference on Mechatronics and Automation (ICMA 2007); 5-8 August 2007; Harbin, China. DOI: 10.1109/ICMA.2007.4304140

[11] Beeby SP, Tudor MJ, White NM. Energy harvesting vibration sources for microsystems applications. Measurement Science and Technology. 2006;**17**:R175-R195

[12] Renaud M, Karakaya K, Sterken T, Fiorini P, Van Hoof C, Puers R. Fabrication, modelling and characterization of MEMS piezoelectric vibration harvesters. Sensors and Actuators A: Physical. 2008;**145-146**:380-386

[13] Epstein AH, Senturia SD. Macro power from micro machinery. Science. 1997;**276**:1211. DOI: 10.1126/science.276.5316.1211

[14] Janicek V, Husak M. Designing the 3D electrostatic microgenerator. Journal of Electrostatics. 2013;**71**:214-219

[15] Holmes AS, Hong G, Pullen KR. Axial-flux permanent magnet machines for micropower generation. Journal of Micro Electro Mechanical Systems. 2005;**14**:54-62

[16] Herrault F, Ji CH, Allen MG. Ultraminiaturized high-speed permanent-magnet generators for milliwatt-level power generation. Journal of Micro Electro Mechanical Systems. 2008;**17**:1376-1387